Operational Tracking of Lava Lake Surface Motion at Kīlauea Volcano, Hawai‘i

Chapter 3 of
Section A, Methods Used in Volcano Monitoring, of
Book 13, Volcano Monitoring

Techniques and Methods 13–A3

U.S. Department of the Interior
U.S. Geological Survey

Cover. Photo of the thermal camera positioned on the rim of Halemaʻumaʻu Crater at the summit of Kīlauea Volcano, Hawaiʻi. The lava lake in the crater has been active since February 2010, and the thermal camera has been in place and continuously running since late 2010. U.S. Geological Survey photograph by Matthew Patrick, taken July 29, 2016.

Operational Tracking of Lava Lake Surface Motion at Kīlauea Volcano, Hawai‘i

By Matthew R. Patrick and Tim R. Orr

Chapter 3 of
Section A, Methods Used in Volcano Monitoring, of
Book 13, Volcano Monitoring

Techniques and Methods 13–A3

U.S. Department of the Interior
U.S. Geological Survey

U.S. Department of the Interior
RYAN K. ZINKE, Secretary

U.S. Geological Survey
William H. Werkheiser, Deputy Director
exercising the authority of the Director

U.S. Geological Survey, Reston, Virginia: 2018

Suggested citation:
Patrick, M.R., and Orr, T., 2018, Operational tracking of lava lake surface motion at Kīlauea Volcano, Hawaiʻi,: U.S. Geological Survey Techniques and Methods 13-A3, 12 p., https://doi.org/10.3133/tm13A3.

ISSN 2328–7055 (online)

Acknowledgments

We thank Jacopo Taddeucci, who introduced us to the PIVlab toolbox, and Einat Lev, who introduced us to the optical flow toolbox. We thank Christoph Kern and another reviewer for constructive reviews. The thermal camera (HTcam) was purchased with funding from the American Recovery and Reinvestment Act (ARRA).

Contents

Figures

Operational Tracking of Lava Lake Surface Motion at Kīlauea Volcano, Hawai‘i

By Matthew R. Patrick and Tim R. Orr

Abstract

Surface motion is an important component of lava lake behavior, but previous studies of lake motion have been focused on short time intervals. In this study, we implement the first continuous, real-time operational routine for tracking lava lake surface motion, applying the technique to the persistent lava lake in Halema‘uma‘u Crater at the summit of Kīlauea Volcano, Hawai‘i. We measure lake motion by using images from a fixed thermal camera positioned on the crater rim, transmitting images to the Hawaiian Volcano Observatory (HVO) in real time. We use an existing optical flow toolbox in Matlab to calculate motion vectors, and we track the position of lava upwelling in the lake, as well as the intensity of spattering on the lake surface. Over the past 2 years, real-time tracking of lava lake surface motion at Halema‘uma‘u has been an important part of monitoring the lake's activity, serving as another valuable tool in the volcano monitoring suite at HVO.

Introduction

The surface motion of a lava lake, which is a fundamental component of its overall behavior, can provide valuable information on processes driving changes within the lake. For example, Harris and others (2005) attributed cycles of surface motion to changing convective regimes within the Erta Ale lava lake in the East African Rift in Ethiopia. Oppenheimer and others (2009) showed that fluctuations in lava lake surface velocity at Mount Erebus were controlled by a pulsatory magma supply entering the lake from deeper levels, and further detailed study of the lake surface behavior by Peters and others (2014a,b) showed that this cyclic activity has persisted for years. Patrick and others (2016a,c) showed that shallowly rooted fluctuations in outgassing (related to spattering) from the lava lake at Kīlauea Volcano produced major changes in lake motion.

Although previous studies have described lava lake motion for limited study periods, here we track lake surface motion continuously in real time, which is important for both monitoring and research. First, unusual changes in lake motion could indicate changes in the deeper magmatic system that might have hazard implications both for Kīlauea's summit and its rift zones. Second, real-time tracking (and timely display of results) bolsters research by providing a continuous "feed" of information that Hawaiian Volcano Observatory (HVO) scientists can view multiple times per day. The constant visibility of these results allows HVO scientists to more easily identify patterns of lava lake behavior and link them with other monitoring parameters, providing a better understanding of volcanic processes in the lake.

In this report, we outline a technique used at the Hawaiian Volcano Observatory to track lava lake surface motion in "Overlook crater," within Halema‘uma‘u Crater at the summit of Kīlauea Volcano, Hawai‘i (fig. 1). The technique analyzes incoming images from a continuously operating thermal camera on the rim of Halema‘uma‘u (fig 2; Patrick and others, 2014) and applies an optical flow approach (Sun and others, 2010) to measure the velocity field. The results are updated in near-real-time on an internal website, thereby building another valuable dataset for HVO's monitoring and research toolkit.

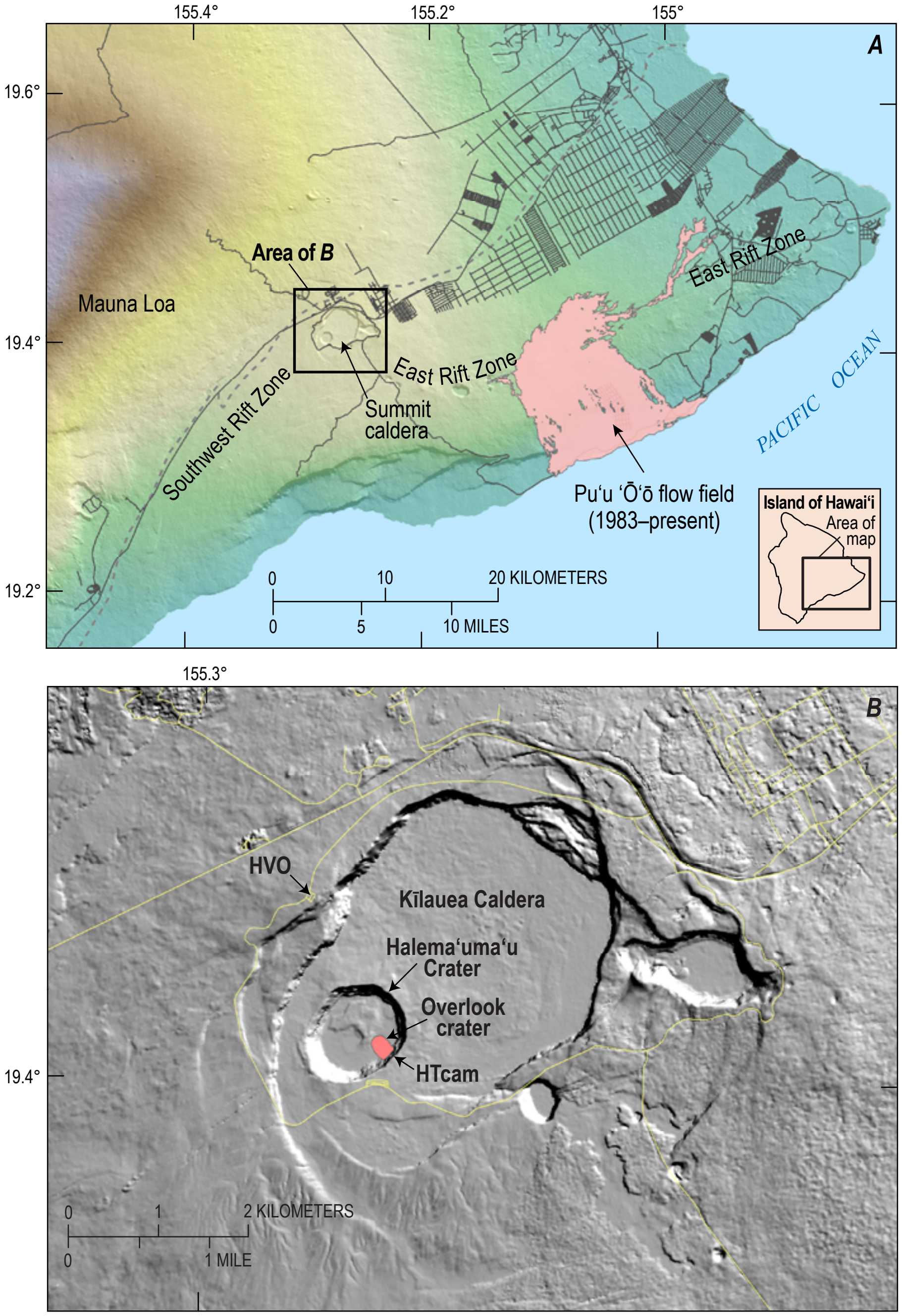

Figure 1. Location map of the summit eruption of Kīlauea Volcano. A, Kīlauea Volcano forms much of the southeast part of the Island of Hawai‘i (see red box in inset for location). The boundary between Mauna Loa (upper left) and Kīlauea is shown by the thick dotted gray line. Kīlauea has two rift zones, the East Rift Zone and the Southwest Rift Zone. The Pu‘u ‘Ō‘ō eruption has been active since 1983 on the East Rift Zone and has created a 144 km^2 lava flow field. The Pu‘u ‘Ō‘ō eruption was concurrent with the summit eruption studied in this report. Black lines are roads. *B*, Shaded-relief map of Kīlauea Caldera (see black box in *A*). The lava lake is contained within the Overlook crater, shown by the light red area. Yellow lines are roads.

Background

Kīlauea’s Summit Eruption

Following several months of increasing seismic tremor and SO_2 emission, Kīlauea’s current summit eruption began on March 19, 2008, with the opening of a new crater on the southeast wall of Halema‘uma‘u Crater (Wilson and others, 2008; Patrick and others, 2013). The new crater, now informally called “Overlook crater,” was initially 35 meters (m) wide and has enlarged through episodic collapses of the crater walls (Orr and others, 2013). Activity in 2008 and 2009 consisted of episodic lava pond activity deep within the crater (about 200 m below the Overlook crater rim), but views of the activity were often obscured by thick fumes. A persistent lava lake began to form in February 2010 as the lava level gradually rose, permitting improved views of the lava surface (Patrick and others, 2015). The lake drained briefly during the March 2011 Kamoamoa event on the East Rift Zone (ERZ; Orr and others, 2015), but reappeared and, after several other ERZ disruptions that affected its lava level, rose higher in 2013. From 2013 to early 2015, the lava lake level was normally 30–60 m below the rim of Overlook crater (fig. 2). In late April and early May 2015, an unusual period of sustained inflation at the summit accompanied rising lava lake level, leading to the lake briefly spilling onto the floor of Halema‘uma‘u Crater during several brief episodes. After a small intrusion,

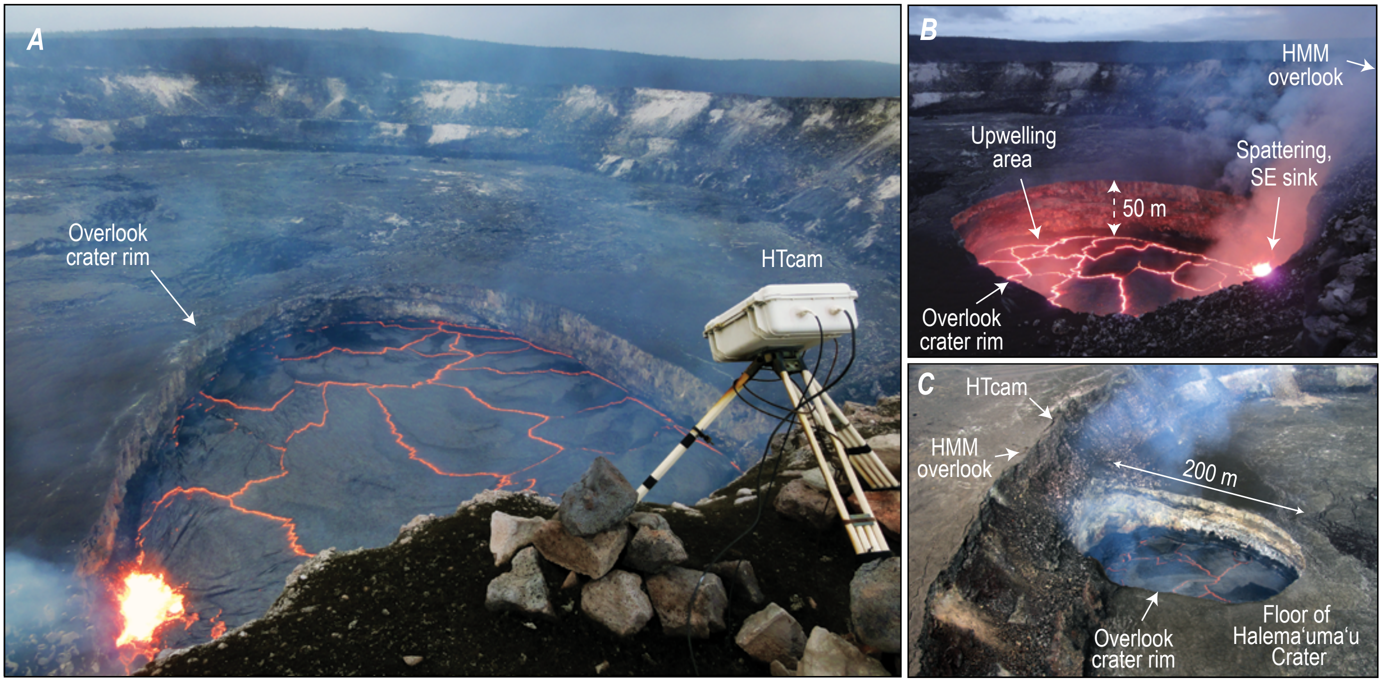

Figure 2. *A*, Photo showing orientation of the thermal camera (HTcam) overlooking the lava lake. The bright yellow area in the bottom left of the photo is a spattering area on the lake margin. Photo taken April 23, 2015. *B*, Photograph of the lava lake taken from 200 meters to the west, on the rim of Halemaʻumaʻu Crater, showing the upwelling area and crustal plates on the surface of the lake. Photo taken February 1, 2014. *C*, Aerial view of the Overlook crater and lava lake, showing locations of the HTcam and Halemaʻumaʻu (HMM) Overlook. Photo taken March 10, 2015.

the lava lake level returned to its more typical levels (30–60 m below Overlook crater rim). In early 2016, the dimensions of Overlook crater were 180 m by 250 m.

Camera Observations of the Lake

The thermal camera system used for velocity measurements was installed at Halemaʻumaʻu in late 2010 and has run continuously since then (fig. 2; Patrick and others, 2014). Automated tracking of lava lake surface velocity, which began within weeks of the camera coming online, consisted of a relatively simple method that we created to track displacement of a single small window on the center of the lake using simple two-dimensional cross-correlation (script H2c in Patrick and others, 2014). Though crude, these results were later corroborated as a fairly good representation of lake surface motion, on the basis of comparison with results using more sophisticated optical flow techniques. Within a year of installation, though, our attention had shifted to other projects, and this motion-tracking algorithm was no longer running.

Automated tracking of the velocity field across the entire lava lake surface, as opposed to at a single measurement window, first became operational in mid-2014. Initially, the routine used the PIVlab Matlab toolbox to perform the calculations (Thielicke and others, 2014). PIVlab performs two-dimensional cross-correlation in small windows throughout the image, and the default configuration results in motion vectors calculated at every 10 row and column pixels. In late 2015, we changed the algorithm to an optical flow routine, specifically the routine originally described by Horn and Schunck (1981) and improved by Sun and others (2010). This new routine had the advantage of calculating motion vectors at every pixel in the image.

Why are thermal cameras used for tracking lava lake surface motion? Visible and near-infrared cameras have varying views of the lake surface because of the thick gas plume produced by lava lake outgassing. At times, the lake surface can be almost completely obscured in images from visible and near-infrared cameras, whereas thermal cameras can “see” effectively through the thick gas, providing an image that is minimally affected by the gas plume (Patrick and others, 2014). Thermal images, therefore, provide a clearer and more continuous picture of the lava lake surface to analyze.

Methodology

Image Acquisition

The lava lake velocity is measured using images from a stationary, continuously operating thermal camera on the rim of Halemaʻumaʻu Crater (Patrick and others, 2014). The Halemaʻumaʻu thermal camera (HTcam) is a Mikron Infrared M7500 model sensitive to longwave infrared (7.5–14 microns) with an image size of 320 by 240 pixels. Because the HTcam is relatively close to the lake, it uses a lens with a wide field of view (horizontal field of view is roughly 53°). Images are collected once every 5 seconds and transmitted to HVO in real-time by Wi-Fi radio. Full details on the HTcam system and image acquisition routine were presented by Patrick and others (2014).

Surface Velocity Vector Measurement

We applied the optical flow approach of Sun and others (2010) to calculate motion vectors across the image, using the Matlab toolbox that is available on that author's web page. This toolbox is a refinement of the optical flow approach of Horn and Schunck (1981), and is the same toolbox used by Lev and others (2012) to measure lava channel motion. The optical flow approach has also been used to track volcanic plume motion (Kern and others, 2015).

We applied the algorithm to image pairs that were three steps (15 seconds) apart, as that interval was long enough to capture very slow motion but not so long as to lose feature matching due to fast velocities. This calculation is performed in 2-minute increments (every 24 images), because processing all images is prohibitively time consuming and produces an excessive amount of data. The algorithm produces images showing vector displacements broken into components u (left to right in the image) and v (up and down in the image), measured in units of pixels.

Converting Image Coordinates to Geographic Coordinates

The optical flow results are in image coordinates (pixels per frame) and need to be converted to geographic coordinates in order to calculate velocity and azimuth. To do so, we used a simple trigonometric projection of the image pixel coordinates onto a horizontal plane, which is represents the lava lake surface. The projection is based on the viewing azimuth and inclination of the HTcam, as measured in the field with a Brunton compass, as well as the HTcam's field of view. We measured the lens distortion for this camera model using the Caltech Matlab camera calibration toolbox created by Jean-Yves Boughet (http://www.vision.caltech.edu/bouguetj/calib_doc/), and found that the lens distortion was very slight—less than 1 percent in areas of the image covered by the lava lake. We therefore assume a rectilinear viewing geometry, using the focal length determined by the calibration toolbox. The calculated geographic positions are in Universal Transverse Mercator coordinates, measured relative to the HTcam position. The easting, northing, and elevation above sea level (geoid corrected) of the HTcam were measured using a kinematic Global Positioning System (GPS) unit. The projection requires knowledge of the vertical distance between the HTcam and the lava lake surface, which is constantly changing because of fluctuations in lava lake level (Patrick and others 2015, 2016a). We use the automated lava level tracking results of Patrick and others (2014, 2016b) to feed hourly estimates of the lava lake level to the velocity tracking routine.

Lava Lake Mask for Velocity Field

Ideally, the motion routine would show zero movement in areas off the lava lake surface, and nonzero vectors on the lava lake surface. In practice, tiny motion vectors show up on the crater walls at times, probably owing to shifting fume creating apparent motion. A simple threshold above these small values would work in most cases, but this approach would discard measurements on the lava lake surface when it is moving very slowly. For these reasons, a more reliable way to filter the results is to apply a mask to the image and collect only those values on the lake surface.

The lava lake mask was constructed each hour, using 1 hour of data (720 images). A composite image was made from these images to show the maximum temperature measured in each pixel position throughout that hour (Patrick and others, 2010). We applied a threshold of 350 °C to create a binary image. To ensure that the mask did not include any of the crater walls, we performed binary erosion on the mask image using a 5-pixel-radius structural element—basically shrinking the mask slightly.

Identifying the Upwelling Area

Visual analysis of time-lapse sequences from the HTcam shows that the lava normally upwells near the northern margin of the lake, and flows south where it downwells at the southern margin (Patrick and others, 2016a,c). Tracking the exact position of this upwelling area is an important part of quantitative tracking of the lake behavior. We used the velocity-vector field to estimate the position of upwelling. A grid search was performed over the lava lake mask to find the pixel that had the best fit as the "origin" of the motion vectors across the lake.

Spattering Intensity

Patrick and others (2016c) showed that spattering activity in the lava lake can strongly influence the surface motion regime. The lava lake surface normally flows toward vigorous spattering sources, where the crust is consumed. During intense spattering episodes, in which spattering occurs along the northern margins of the lava lake, the surface flow direction can completely reverse, which Patrick and others (2016c) called "spattering-driven" surface flow behavior. Because of the association between spattering and lava lake motion, measuring spattering intensity through time is a useful addition to monitoring lake surface motion.

We take a simple approach to tracking spattering intensity and simply measure the area of spattering in the image. Spattering almost always saturates the pixels, which have a peak temperature of 500 °C, and so we apply a threshold of 499 °C to the image to produce a binary image that shows the saturated pixels. This binary image sometimes contains narrow bands where high temperatures are present in the incandescent spreading zones between crustal plates, and so we apply a morphologic opening filter (Gonzalez and others, 2004) with a one-pixel-radius structural element to minimize the effect of these spreading zones. The resulting spattering pixels are then converted to area on the basis of pixel size, which is calculated using the algorithm for conversion between image coordinates and geographic coordinates.

Displaying Results

A clear, timely display of monitoring results is needed to use the data in an operational routine. Our algorithm produces an hourly update on the lave lake motion in the form of a web page "dashboard" that includes images and plots of the data, all fitting within the area of a single screen (fig. 3), including:

1. A recent example thermal image of the lava lake, overlain by motion vectors, provides a qualitative picture of current lake motion.

2. Histograms summarizing velocities over the past month for (a) all periods, (b) spattering regimes, and (c) nonspattering regimes. The spattering and nonspattering regimes are discriminated using a real-time seismic

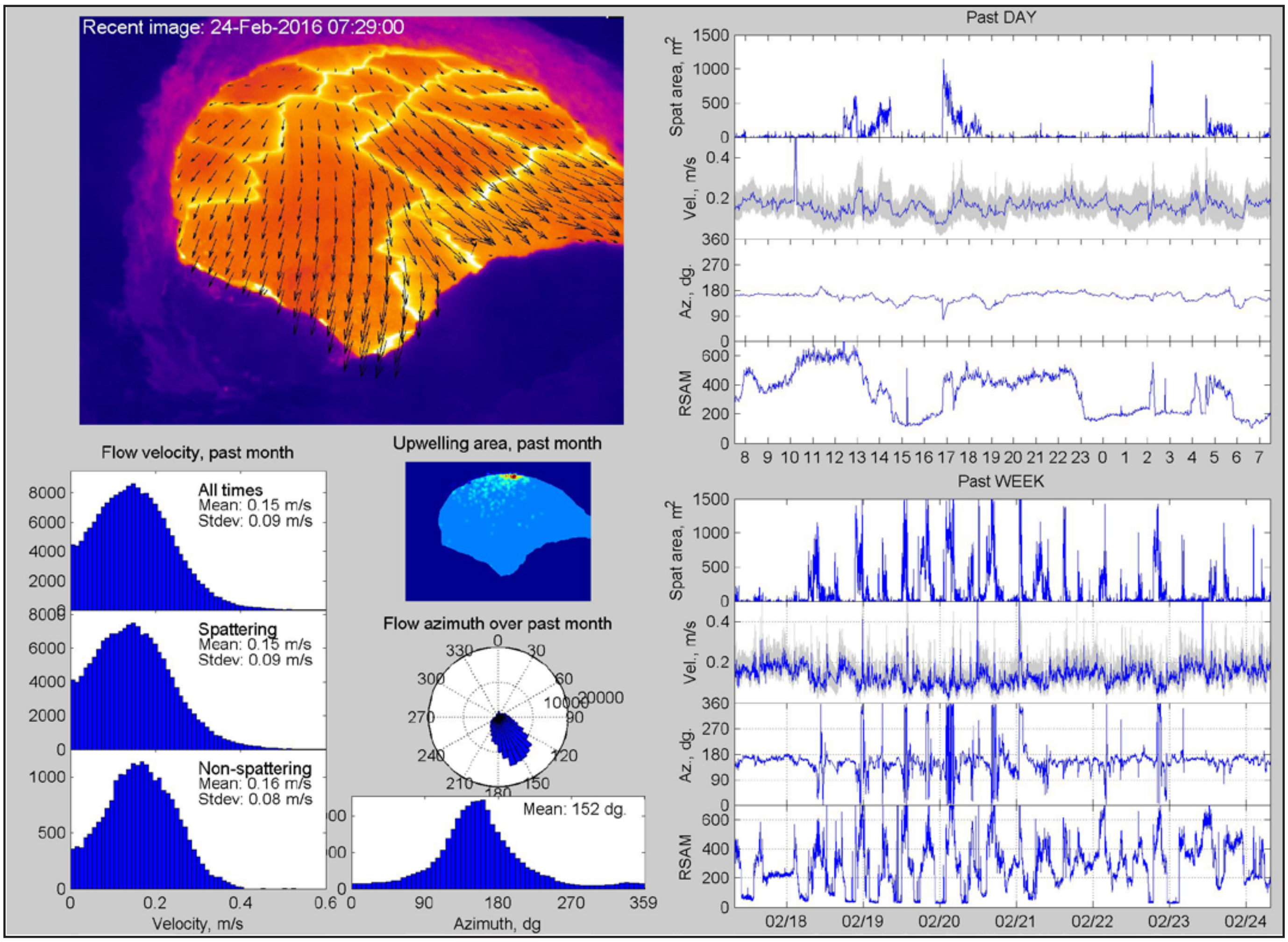

Figure 3. Example screenshot of the automated "dashboard" that shows results of lava lake motion measurements, updated hourly on the Hawaiian Volcano Observatory internal website. Upper left, recent thermal image with flow vectors to qualitatively show recent lava lake activity. White and yellow colors are hottest areas; blue and purple are cooler and show the crater walls. Lower left, three histograms showing distribution of surface velocity over the past month for (top) all times, (middle) times of spattering activity and (bottom) times of nonspattering activity. The y axis in these histograms is number of measurements. The velocity histograms also summarize the mean velocity in each plot (in meters per second, m/s), and the standard deviation (stdev, also given in m/s). The upwelling site solutions for the past month are shown left of center, showing hot colors where upwelling site is most commonly located. The lava lake mask is shown by the light blue color. Below left of center, surface flow azimuths are shown by a rose diagram and conventional histogram. The most common flow azimuth is about 150° (southeast), which represents stable, upwelling-driven flow. Upper right, stacked plots show lava lake activity over the past day, including spattering area (in square meters, m^2), surface velocity (in meters per second, m/s; mean is blue line; gray area is one standard deviation), mean flow azimuth (in degrees) and RSAM (real-time seismic amplitude measurements). Nonspattering phases of lava lake activity are evident by low, flat RSAM values, while peak RSAM values correspond to increases in spattering activity. Lower right, the same data are shown for the past week.

amplitude measurement (RSAM) threshold (Patrick and others, 2016a). These histograms consider the varying pixel footprint size across the lava lake and weight the data accordingly.

3. A rose plot and normal histogram showing flow azimuths over the past month. Again, weighting is done to account for the different pixel footprint sizes across the lava lake.

4. An image and map showing the position of the upwelling area over the past month.

5. A time-series plot of mean velocity (and its standard deviations) over the past day and week.

6. A time-series plot of mean flow azimuth over the past day and week. The mean azimuth is calculated using the standard technique for circular quantities, which involves converting the angles to points on the unit circle.

7. A time-series plot of RSAM over the past day and week, which shows tremor fluctuations corresponding to changes in spattering and nonspattering regimes. RSAM is measured from broadband station NPT after highpass filtering (>1 Hertz) of the data. The RSAM data are pulled from HVO's data server by a JavaScript Object Notation (JSON) interface in MATLAB, using the JSONlab toolbox (Fang and Boas, 2009). Previous work (Kern and others, 2015; Nadeau and others, 2015; Patrick and others 2016a,c) shows that this high-frequency seismic tremor correlates strongly with gas emission rates and can be used as a rough proxy for gas emission rate.

An image mosaic on the HVO internal web server displays hourly images from the past 24 hours (fig. 4). These images, which have the motion vectors superimposed to show a sequential qualitative picture of recent lake motion, are particularly useful to see how changes in the vigor and location of spattering can influence lava lake surface motion.

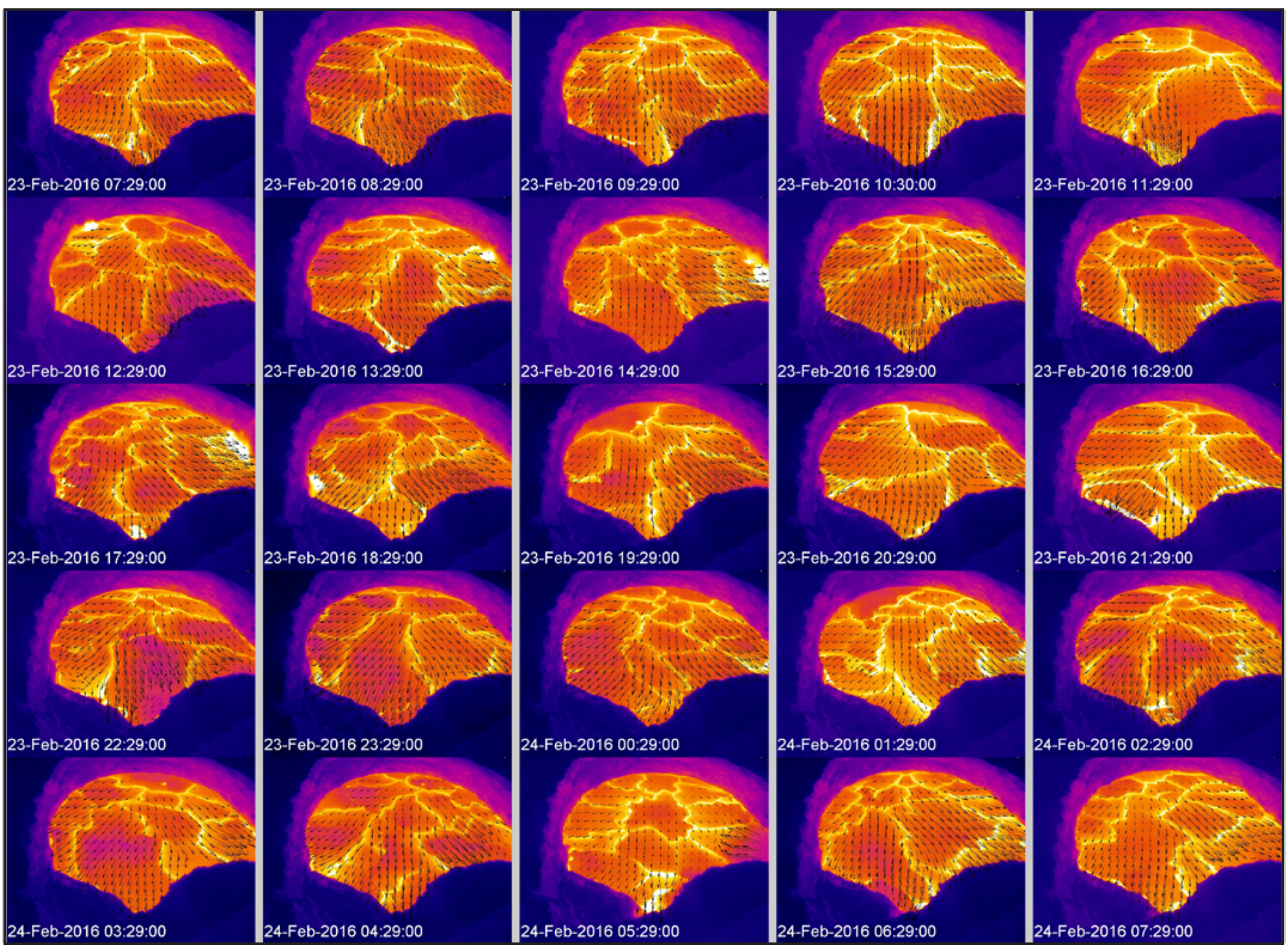

Figure 4. Example screenshot of the automated image mosaic that is updated hourly on the Hawaiian Volcano Observatory internal website. Images are selected from each hour over the past 24 hours and motion vectors are overlain on the thermal images, which are useful for getting a qualitative sense of recent activity. White and yellow areas are hottest; blue and purple are cooler and show the crater walls.

The mean and standard deviation of velocity and mean of the flow azimuth are calculated in 2-minute intervals and exported each hour into a text file that is readable by VALVE, a web-based interface that displays real-time monitoring data (fig. 5; Cervelli and others, 2002). VALVE, which is used at several USGS volcano observatories, is an integral part of the monitoring routine because by exporting the velocity and azimuth data into VALVE, the results of the lava-lake surface velocity calculations can easily be compared with other datasets, such as RSAM or SO_2 emissions.

Processing Flow

Images of the lava lake are collected every 5 seconds and saved to an acquisition folder as they are acquired. Once every hour, a MATLAB script runs automatically and copies the images from the acquisition folder into a temporary folder for analysis (script 1 in appendix 1), which includes (1) a lava level estimation (Patrick and others, 2016b); (2) a velocity measurement (script 2 in appendix 1); (3) upwelling position estimation (script 3 in appendix 1); and (4) spatter area tracking (script 4 in appendix 1). The velocity measurements, upwelling position estimates, and spattering data are saved in hourly files. Each hour, another MATLAB script (script 6 in appendix 1) reads the hourly files over the past month and produces the "dashboard" image that is sent to the HVO internal web server. Once the analysis scripts are finished, the images in the temporary folder are then archived in a date-based folder structure (script H2d in Patrick and others, 2014). These MATLAB scripts are run automatically using a program called System Scheduler (produced by Splinterware software), as this program proved more reliable than the default Windows Scheduler program.

Sources of Error

The optical flow method we use (that of Sun and others, 2010) has been tested and compared with other optical flow algorithms on the Middlebury Benchmark site (http://vision.middlebury.edu/flow/; also see Baker and others, 2011). As of

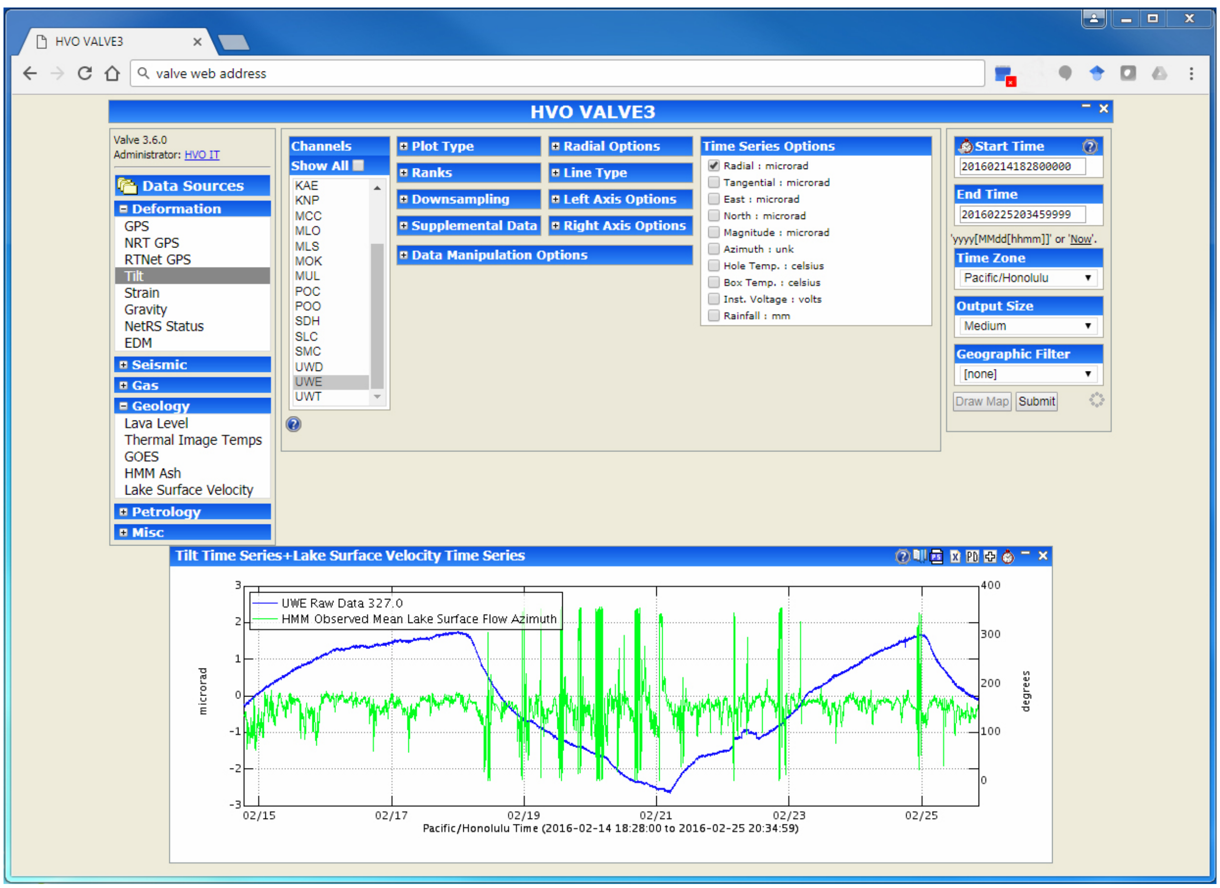

Figure 5. Screenshot of the VALVE interface. VALVE is a web-based program used by U.S. volcano observatories to integrate real-time monitoring data (Cervelli and others, 2002). Here, the green line shows mean lava surface flow direction and the blue line shows summit ground tilt (radial component at station UWE). Decreasing values of ground tilt indicate summit deflation, and increasing values show inflation. The flow direction shows an increase in the number of flow reversals (unstable, spattering-driven regimes shown by green spikes) during summit deflation. This pattern is commonly observed at Halema'uma'u. As Patrick and others (2016c) show, summit deflation is associated with a drop in the lake level, which triggers small collapses from Overlook crater walls that impact the lake, often triggering spattering along the north margin of the lake. Spattering along the north margin can shift the lava lake into an unstable flow regime because of the tendency of the lava lake surface to flow toward, and plunge into, spattering sources.

October 2016, the algorithm was ranked 28 of 122 for endpoint error and 31 of 122 for angular error, and thus is in the top third of algorithms tested.

Besides the flow-measurement algorithm itself, an obvious source of error is in the conversion of image measurements (pixels per frame) to physical units (meters per second and degrees), which requires a projection of the image geometry onto the lava lake surface that, in turn, depends on an estimate of lava lake surface elevation, which is done using an automated lava level routine based on the thermal images, along with an empirical conversion based on sporadic laser-rangefinder measurements (Patrick and others, 2016b). Patrick and others (2016b) compared the estimated elevations with laser rangefinder measurements and showed that there was a root-mean-square error of 1.5 m. The laser rangefinder measurements themselves have an error of ±1 m, and, assuming that the total error is the square root of the sum of the squared individual errors (1.5 and 1 m), then the total error is ±1.8 m. Rounding up to an assumed lava-lake level error of ±2 m, we calculated the resulting error in terms of mean velocity and mean azimuth using a test dataset from March 24, 2015, when the lake was about 50 m below the Overlook crater rim. The velocity change in this case was roughly 1.5 percent, and the angular error was <1°. Assuming larger errors in the lava lake elevation, of ±4 m, results in velocity errors of about 3 percent. Overall, even moderate errors (several meters) in lava lake surface elevation produce relatively minor errors in estimates of lava lake surface velocity and flow direction.

Another potential source of error is associated with saturated pixels in the image (where the lava lake surface temperature is >500 °C). The script is unable to measure surface velocities in these zones because there is no measured temperature contrast in the saturated areas. These areas, which are typically zones of spattering, normally cover a small fraction of the total lava lake area, and so their absence in the velocity results should be insignificant. Furthermore, this technique is more focused on the motion of the crustal plates that move across the surface of the lava lake and not on the chaotic motion of the spattering zones.

Finally, the finite size of pixels in the image may limit the precision with which lava lake motion can be measured. The pixel footprint size over the lake is generally 0.5–3 m^2, which probably provides a reasonable approximation of lake motion by the large crustal plates (each tens of square meters in size, covering most of the lake's surface), but may not depict the small-scale motion at crustal spreading zones and around spattering sites.

Results

Patrick and others (2016a) describes the lava lake's two outgassing regimes: spattering and nonspattering. At most times, including both spattering and nonspattering activity, the lava-lake surface motion is relatively stable, moving from the upwelling source at the northern margin of the lake towards the southern margin, where lava sinks. Patrick and others (2016c) characterize this "stable" north-south flow as being upwelling-driven (fig. 6). During some periods, however, commonly when vigorous spattering is present along the northern margin of the lake, the flow can reverse, with crust drawn towards the spattering, where it downwells in an "unstable" flow regime that is spattering driven. Unstable flow is not strictly northward, and the flow direction depends on the spattering location; sometimes the flow splits and moves toward multiple spattering areas simultaneously. Patrick and others (2016c) showed how these stable and unstable flow regimes have characteristic directions and outgassing intensities. The unstable, spattering-driven behavior, which is shallowly rooted in the lake, is an interruption to the more deeply seated, stable, upwelling-driven flow.

The shifting behavior of the lava lake, between stable and unstable flow regimes, can be shown using the automated motion tracking results (data replotted in fig. 7). Most of the time spattering along the north margin of the lake is inactive, and the lava lake is in a stable flow regime (fig. 7*A*), characterized by relatively steady flow direction centered around an azimuth of 150° (fig. *7D*). When spattering along the north margin of the lake is strong, however, the flow direction abruptly changes, usually reversing to flow northward, toward the spattering sources. Seven or eight of these unstable flow episodes occurred in the study period from February 18 to 20, 2016. Though Patrick and others (2016c) shows how unstable flow regimes are often associated with a reduction in surface flow velocities, this association was not strong during this study period (fig. 7*E*). Periods of spattering along the north margin of the lava lake are evident by increases in seismic tremor at the summit, shown by peaks in RSAM (fig. 7*F*).

These same relations are also evident in the automated dashboard plot of results (fig. 3). Focusing on the "past week" data (lower right panes, fig. 3), there were many episodes of spattering, the largest of which were associated with shifts in flow direction and peaks in RSAM data that characterized unstable flow behavior. These relatively brief unstable phases, however, interrupted the general trend in flow azimuth, which was relatively steady at about 150° and characterized stable flow. The relation between flow direction and spattering location is also shown well by the automated image summary (fig. 4).

Unstable flow regimes appear to be more common during summit deflation, as suggested by the example VALVE plot (fig. 5) and many other observations. Summit deflation is associated with a drop in lava lake level (Patrick and others, 2015), which often triggers small collapses of the lava veneer that adheres to the Overlook crater walls. These collapses impact the lake and trigger spattering, and these spattering sources can then cause surface flow reversals and unstable flow behavior (Patrick and others, 2016c).

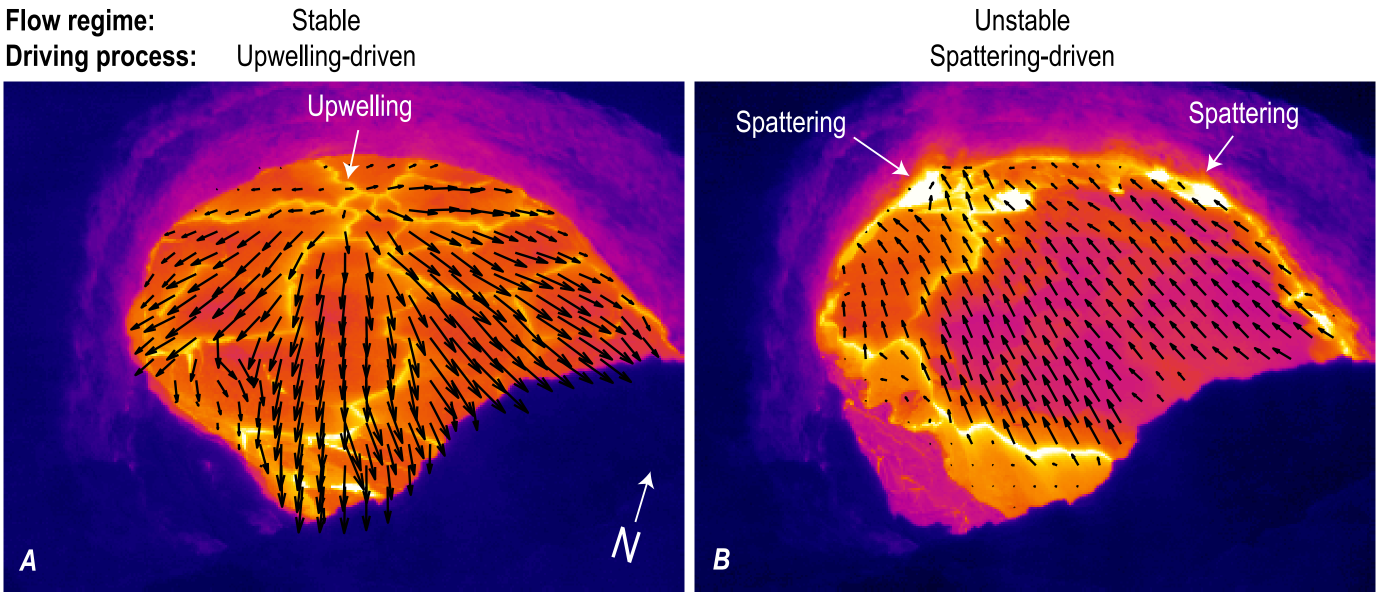

Figure 6. Comparison of lava lake surface flow regimes at Halemaʻumaʻu (modified from Patrick and others, 2016c). Stable surface flow (or nonspattering, *A*) is from north to south, driven by upwelling in the northern part of the lake. Unstable surface flow (*B*) varies, as crust is drawn toward spattering sources on the lava lake margin. Unstable flow direction is commonly toward the north—a reversal in flow direction relative to stable flow regimes. Unstable behavior is spattering-driven, and is a shallow interruption to the more deeply-seated, upwelling-driven flow.

Discussion

The automated results from the method described here add much greater depth to the study of lava lake surface motion, in comparison to brief campaign-style data collection. Automated results provide a large volume of continuous, long-term data that can be mined to identify trends and patterns and compare with geophysical data. Patrick and others (2016c) describe the different regimes of surface flow, alternating between stable, upwelling-driven flow and unstable, spattering-driven flow. Although that study includes several short time series as examples, the conceptual model arose from numerous, often incidental, views of the real-time continuous velocity field results shown here. This comparison is just one example of the benefit of continuous, automated processing that "pushes" results to the observatory scientist, as opposed to the more time-consuming and sporadic approach of manually "pulling" data for processing.

The data produced from this algorithm provides one of the best opportunities worldwide to understand lava lake motion. Future studies could involve analyzing the long-term (multiyear) trends and comparing them with long-term changes in deformation and outgassing rates. These data may also serve as a valuable foundation for computational modeling of lava lake dynamics, which would be needed to infer deeper processes from the surface motion.

Conclusions

In this study, we describe an operational approach to quantitatively track lava lake surface motion at Halemaʻumaʻu Crater on Kīlauea Volcano, Hawaiʻi. The velocity field is measured from thermal images, and other image processing techniques are used to measure spattering intensity. We show that automated tracking of lava lake surface motion provides a useful technique to augment the existing suite of monitoring tools at the Hawaiian Volcano Observatory.

Routine monitoring of lava lake activity in Hawaiʻi began in 1911 (Perret, 1913), and continued for more than a decade

Figure 7. Example of results from the automated script, which collects surface motion data from the thermal images and calculates spattering area, flow direction, and flow velocity. The thermal images (*A* and *B*) show how the appearance of the lake changes as the flow regime changes. White areas are hottest; blue and purple areas are crater walls. Data in *C*–*F* replotted from a study period from February 17 to 20, 2016. Stable surface flow activity (*A*) involves the surface flowing southward (roughly 150° mean azimuth) and is associated with either no spattering or minor/moderate spattering. Unstable flow regimes (*B*) are triggered by episodes of intense spattering (*C*), which can trigger abrupt changes in a flow direction (*D*). In these examples, surface flow velocity (*E*) shows only minor changes related to stable-unstable transitions. Increased spattering is normally associated with increased seismic tremor, shown by peaks in the real-time seismic amplitude measurements (RSAM; *F*). Red dashed lines correspond to when thermal images in *A* and *B* were collected.

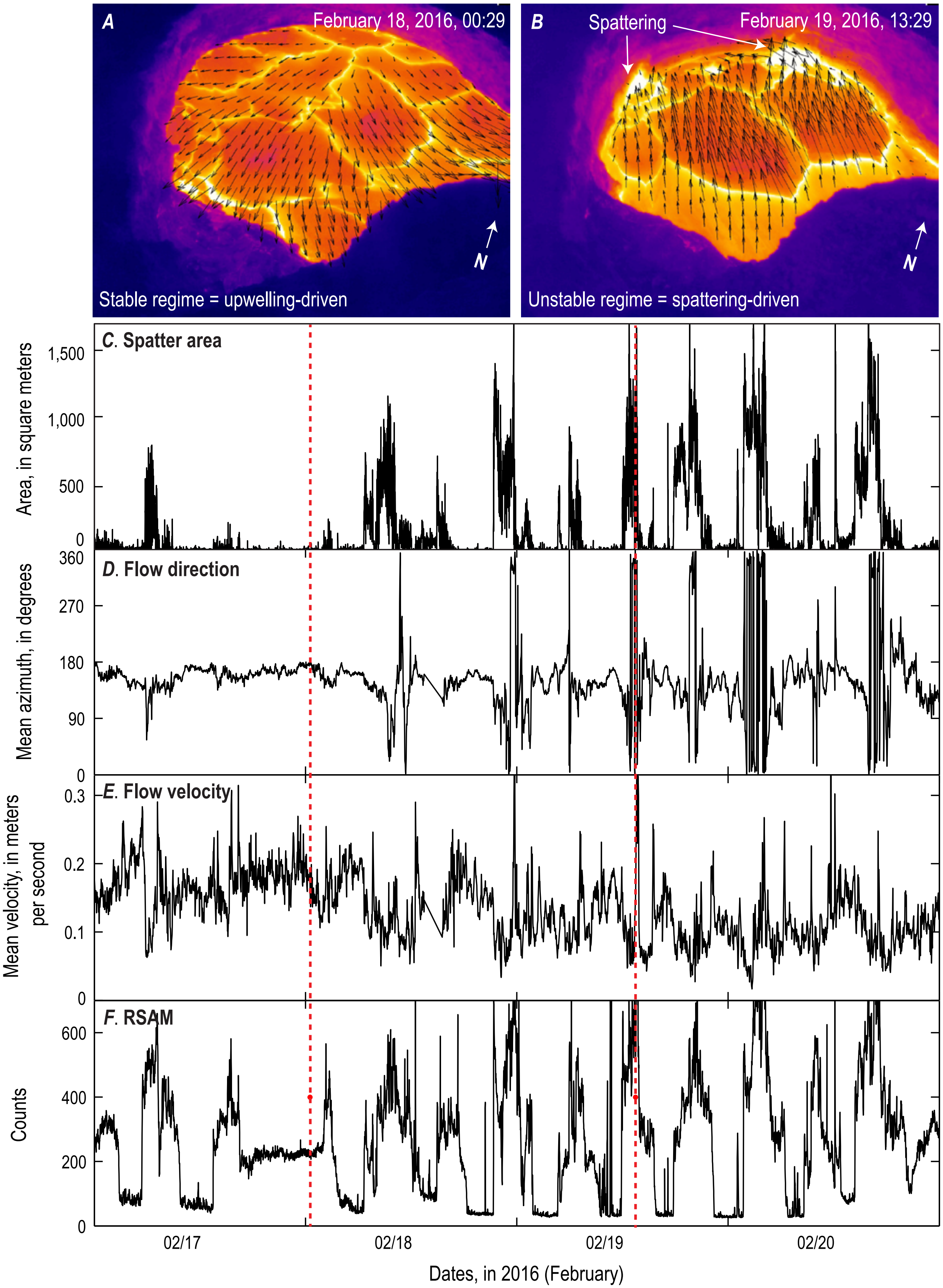
A
February 18, 2016, 00:29
N
Stable regime = upwelling-driven
B
Spattering
February 19, 2016, 13:29
N
Unstable regime = spattering-driven
C. Spatter area
Area, in square meters
1,500
1,000
500
0
D. Flow direction
Mean azimuth, in degrees
360
270
180
90
0
E. Flow velocity
Mean velocity, in meters per second
0.3
0.2
0.1
0
F. RSAM
Counts
600
400
200
0
02/17
02/18
02/19
02/20
Dates, in 2016 (February)

after establishment of the Hawaiian Volcano Observatory (HVO) in 1912 (Jaggar, 1947). This observational dataset was terminated by the end of lava lake activity in 1924. As Patrick and others (2016c) describes, HVO scientists during that time observed and documented many of the fundamental conceptual relations among spattering activity, outgassing, lake surface motion, and seismic tremor. However, the technological limitations of that era limited the degree to which lava lake activity could be quantitatively measured. Today, thermal cameras in combination with sophisticated image processing techniques provide an exceptional degree of rigor in characterizing how lava lakes behave (Peters 2014a,b), and we show how these tools can be combined to work in an automated fashion. The volume and quality of these data afford new opportunities for understanding the processes that drive lava lake activity.

References Cited

Baker, S., Scharstein, D., Lewis, J.P., Roth, S., Black, M.J., and Szeliski, R., 2011, A database and evaluation methodology for optical flow: International Journal of Computer Vision, v. 92, p. 1–31. [Also available online at https://link.springer.com/content/pdf/10.1007%2Fs11263-010-0390-2.pdf]

Cervelli, D.P., Cervelli, P.F., Miklius, A., Krug, R., and Lisowski, M., 2002, VALVE; volcano analysis and visualization environment [abs.]: Eos, Transactions, American Geophysical Union, v. 83, no. 47, Fall meeting supplement, abs. U52A-01.

Fang, Q., and Boas, D., 2009, Tetrahedral mesh generation from volumetric binary and gray-scale images: Institute of Electrical and Electronics Engineers [IEEE], Proceedings of the 6th IEEE International Symposium on Biomedical Imaging—From nano to macro, 2009, p. 1142–1145.

Gonzalez, R.C., Woods, R.E., and Eddins, S.L., 2004, Digital image processing using MATLAB®: Upper Saddle River, New Jersey, Pearson-Prentice Hall.

Harris, A.J.L., Carniel, R., and Jones, J., 2005, Identification of variable convective regimes at Erta Ale lava lake: Journal of Volcanology and Geothermal Research, v. 142, p. 207–223. [Also available online at http://www.sciencedirect.com/science/article/pii/S0377027304003737]

Horn, B., and Schunck, B., 1981, Determining optical flow: Artificial Intelligence, v. 16, p. 185–203.

Jaggar, T.A., 1947, Origin and development of craters: Geological Society of America Memoir 21, 508 p.

Kern, C., Sutton, J., Elias, T., Lee, L., Kamibayashi, K., Antolik, L., and Werner, C., 2015, An automated SO_2 camera system for continuous, real-time monitoring of gas emissions from Kilauea Volcano's summit Overlook: Journal of Volcanology and Geothermal Research, v. 300, p. 81–94. [Also available online at http://www.sciencedirect.com/science/article/pii/S0377027314003783]

Lev, E., Spiegelman, M., Wysocki, R.J., and Karson, J.A., 2012, Investigating lava flow rheology using video analysis and numerical analysis: Journal of Volcanology and Geothermal Research, v. 247, p. 62–73. [Also available online at http://www.sciencedirect.com/science/article/pii/S0377027312002405]

Nadeau, P.A., Werner, C.A., Waite, G.P., Carn, S.A., Brewer, I.D., Elias, T., Sutton, A.J., and Kern, C., 2015, Using SO_2 camera imagery and seismicity to examine degassing and gas accumulation at Kilauea Volcano, May 2010: Journal of Volcanology and Geothermal Research, v. 300, p. 70–80, doi:10.1016/j.jvolgeores.2014.12.005. [Also available online at http://www.sciencedirect.com/science/article/pii/S0377027314003795]

Oppenheimer, C., Lomakina, A.S., Kyle, P.R., Kingsbury, N.G., and Boichu, M., 2009, Pulsatory magma supply to a phonolite lava lake: Earth and Planetary Science Letters, v. 284, p. 392–398. [Also available online at http://www.sciencedirect.com/science/article/pii/S0012821X09002805]

Orr, T.R., Thelen, W.A., Patrick, M.R., Swanson, D.A., and Wilson, D.C., 2013, Explosive eruptions triggered by rockfalls at Kilauea Volcano, Hawai‘i: Geology, v. 41, p. 207–210. [Also available online at https://pubs.geoscienceworld.org/geology/article-lookup/41/2/207]

Orr, T.R., Poland, M.P., Patrick, M.R., Thelen, W.A., Sutton, J., Elias, T., Thornber, C.T., Parcheta, C., and Wooten, K.M., 2015, Kīlauea's 5-9 March 2011 Kamoamoa fissure eruption and its relation to 30+ years of activity from Pu‘u ‘Ō‘ō, chap. 18 *of* Carey, R., Poland, M., Cayol, V., Weis, D., eds., Hawaiian Volcanism—From Source to Surface: American Geophysical Union Geophysical Monograph 208, p. 393–420.

Patrick, M.R., Kauahikaua, J., and Antolik, L., 2010, MATLAB tools for improved characterization and quantification of volcanic incandescence in webcam imagery—applications at Kīlauea Volcano, Hawai‘i: U.S. Geological Survey Techniques and Methods 13-A1, 16 p. [Also available online at https://pubs.usgs.gov/tm/tm13a1/tm13a1.pdf]

Patrick, M.R., Orr, T., Sutton, A.J., Elias, T., and Swanson, D., 2013, The first five years of Kīlauea's summit eruption in Halema‘uma‘u, 2008–2013: U.S. Geological Survey Fact Sheet 2013–3116, 4 p., https://dx.doi.org/10.3133/fs20133116.

Patrick, M.R., Orr, T., Antolik, L., Lee, L., and Kamibayashi, K., 2014, Continuous monitoring of Hawaiian volcanoes with thermal cameras: Journal of Applied Volcanology, v. 3, no. 1, accessed November 2017 at https://link.springer.com/article/10.1186/2191-5040-3-1.

Patrick, M.R., Anderson, K.R., Poland, M.P., Orr, T., and Swanson, D., 2015, Lava lake level as a gauge of magma reservoir pressure and eruptive hazard: Geology, v. 43, p. 831–834. [Also available online at https://pubs.geoscienceworld.org/geology/article-lookup/43/9/831]

Patrick, M.R., Orr, T., Sutton, A.J., Lev, E., and Fee, D., 2016a, Shallowly driven fluctuations in lava lake outgassing, Kīlauea Volcano, Hawai‘i: Earth and Planetary Science Letters, v. 433, p. 326–338. [Also available online at http://www.sciencedirect.com/science/article/pii/S0012821X15006883]

Patrick, M.R., Orr, T., and Swanson, D., 2016b, Automated tracking of lava lake level using thermal images at Halema‘uma‘u Crater, Kīlauea Volcano: Journal of Applied Volcanology, v. 5, no. 6, accessed November 2017 at https://appliedvolc.springeropen.com/articles/10.1186/s13617-016-0047-0.

Patrick, M.R., Orr, T., Swanson, D., Lev, E., 2016c, Shallow and deep controls on lava lake surface motion, Kīlauea Volcano: Journal of Volcanology and Geothermal Research, v. 328, p. 247–261, http://dx.doi.org/10.1016/j.jvolgeores.2016.11.010. [Also available online at http://www.sciencedirect.com/science/article/pii/S0377027316304590]

Perret, F.A., 1913, The circulatory system in the Halemaumau lake during the summer of 1911: American Journal of Science, ser. 4, v. 35, p. 273–282.

Peters, N., Oppenheimer, C., Killingsworth, D.R., Frechette, J., and Kyle, P., 2014a, Correlation of cycles in lava lake motion and degassing at Erebus Volcano, Antarctica: Geochemistry, Geophysics, Geosystems, v. 15, no. 8, p. 3244–3257, doi:10.1002/2014GC005399, accessed November 2017 at http://onlinelibrary.wiley.com/doi/10.1002/2014GC005399/full.

Peters, N., Oppenheimer, C., Kyle, P., and Kingsbury, N., 2014b, Decadal persistence of cycles in lava lake motion at Erebus volcano, Antarctica: Earth and Planetary Science Letters, v. 395, p. 1–12. [Also available online at http://www.sciencedirect.com/science/article/pii/S0012821X14001848]

Sun, D., Roth, S., and Black, M., 2010, Secrets of optical flow estimation and their principles: Institute of Electrical and Electronics Engineers [IEEE], IEEE Conference on Computer Vision and Pattern Recognition (CVPR), 2010, p. 2432–2439. [Also available online at http://ieeexplore.ieee.org/abstract/document/5539939/figures]

Thielicke, W., and Stamhuis, E.J., 2014, PIVlab—Towards user-friendly, affordable and accurate digital particle image velocimetry in MATLAB: Journal of Open Research Software, v. 2, no. 1, e30, http://dx.doi.org/10.5334/jors.bl. [Also available online at https://openresearchsoftware.metajnl.com/articles/10.5334/jors.bl/]

Wilson, D., Elias, T., Orr, T., Patrick, M., Sutton, A.J., and Swanson, D., 2008, Small explosion from new vent at Kīlauea’s summit: Eos, Transactions, American Geophysical Union, v. 89, p. 203. [Also available online at http://onlinelibrary.wiley.com/doi/10.1029/2008EO220003/full]

Menlo Park Publishing Service Center, California
Manuscript approved for publication December 11, 2017
Edited by George Havach and Claire Landowski
Layout and design by Cory D. Hurd

Patrick and Orr—**Operational Tracking of Lava Lake Surface Motion at Kīlauea Volcano, Hawai'i**—Techniques and Methods 13–A3

ISSN 2328–7055 (online)
https://doi.org/10.3133/tm13A3